Merged molecular switches excel as optoacoustic dyes: azobenzene-cyanines are loud and photostable NIR imaging agents

Markus Müller[a], Nian Liu[b,c], Vipul Gujrati[b,c], Abha Valavalkar[d,e], Sean Hartmann[f], Andras Telek[a], Benjamin Dietzek-Ivanšić[d,e], Achim Hartschuh[f], Vasilis Ntziachristos[b,c], Oliver Thorn-Seshold[a]*

[a] Department of Pharmacy, LMU Munich, Butenandtstrasse 7, Munich 81377, Germany; *oliver.thorn-seshold@cup.lmu.de

[b] Institute of Biological and Medical Imaging, Helmholtz Zentrum München, Ingolstaedter Landstrasse 1, Neuherberg 85764, Germany.

[c] Chair of Biological Imaging at the Central Institute for Translational Cancer Research (TranslaTUM), School of Medicine, Technical University of Munich, Ismaninger Str. 22, Munich 81675, Germany.

[d] Institute of Physical Chemistry, University of Jena, Lessingstraße 4, Jena 07743, Germany.

[e] Leibniz Institute of Photonic Technology Jena, Research Department Functional Interfaces, Albert-Einstein-Straße 9, Jena 07745 Germany.

[f] Department of Chemistry, LMU Munich, Butenandtstrasse 8, Munich 81377, Germany.

KEYWORDS: optoacoustic imaging, photoacoustic dye, photoswitch, fluorescence, quencher

ABSTRACT: Optoacoustic imaging, also known as photoacoustic imaging, promises micron-resolution noninvasive imaging in biology at much deeper penetration (>cm) depths than e.g. fluorescence. However, the loud, photostable, NIR-absorbing molecular contrast agents which would be needed for optoacoustic imaging of enzyme activity remain unknown: most organic molecular contrast agents are simply repurposed fluorophores, with severe shortcomings of photoinstability or phototoxicity under optoacoustic imaging conditions, which are consequences of their slow $S_1 \rightarrow S_0$ electronic relaxation rates. We now disclose that known fluorophores can be rationally modified to reach ultrafast $S_1 \rightarrow S_0$ rates, without much extra molecular complexity, simply by merging them with molecular switches. Here, we merge azobenzene switches to cyanine dyes to give ultrafast relaxation (<10 ps, >100-fold faster). Even without adapting instrument settings, these azohemicyanine optoacoustic imaging agents deliver outstanding improvements in signal longevity (>1000-fold increase of photostability) and signal loudness (here: >3-fold even at time zero). We show why this still-unexplored design strategy can offer even stronger performance in the future, as a simple method that will also increase the spatial resolution and the quantitative linearity of photoacoustic response even over extended longitudinal imaging. By bringing the world of molecular switches and rotors to bear on unsolved problems that have faced optoacoustic agents, this practical strategy may be a crucial step towards unleashing the full potential, in fundamental studies and in translational uses, of optoacoustic imaging.

INTRODUCTION

The idea of designing chromophores for ultrafast $S_1 \rightarrow S_0$ electronic relaxation has not yet been raised as a goal for optimising NIR optoacoustic contrast agents, but we feel it will be crucial for successful translation of optoacoustic imaging. Here, we bring it to the community, by showing how a simple design lowers $S_1 \rightarrow S_0$ lifetimes by >100-fold, and thus improves far beyond current limits of signal loudness (here: >3-fold) and dye photostability (>1000-fold).

Optoacoustic imaging, interchangeably called photoacoustics or "PA", adds new opportunities to the imaging toolbox. In PA, short laser pulses excite optical absorbers; when they locally dissipate the excitation energy as heat during the pulse, an expansion pressure wave results, that can be detected with low attenuation and high localisation by ultrasound transducers.[1] With its unique optical-input/acoustic-output combination, PA offers attractive features that other imaging techniques do not: PA penetrates several cm through tissue, with resolution down to 150 μm, and can image endogenous or exogenous contrast agents (by MSOT, multispectral optoacoustic tomography).[2,3] Thus, PA has become valuable particularly in anatomical imaging, from basic research[4] to image-guided surgery.[5]

PA's ultrasound output has excellent tissue penetration; its depth limits come from its optical input. NIR light suffers the least during tissue penetration,[6] so PA adopted NIR dyes as exogenous contrast agents. Cyanine (Cy) dyes played a major role[7] because of their strong NIR absorption and their rational wavelength tuning capacities, that had been developed for fluorescence.[8] In particular, as the Cy dye indocyanine green (**ICG**) is FDA-approved for fluorescence imaging, it was rapidly adopted in PA and is still widely used.[9,10]

Cyanines are still very actively researched: e.g. as SWIR (1-2 μm) fluorophores enabling deeper tissue penetration,[11–13] or as hybrid "hemicyanine" structures[14] that are easier to make into fluorogenic[15] or acoustogenic[16–18] probes. Other fluorophore and PA contrast agent structural scaffolds have been excellently reviewed.[7,19]

However, there has been little rational development of contrast agents to optimise the specific properties needed for PA; in fact, principles for best PA are not even widely agreed upon. Thus, accessible fluorophores, such as Cy dyes, continue to be widely used even though the properties that make them good fluorophores lead to diverse problems when used in PA. These issues have been well-reviewed by Rochford.[20] An optoacoustic signal is proportional to the fraction of absorbed optical energy which is dissipated as heat by vibrational relaxation (VR). An obvious drawback of good fluorophores is that they undergo fast VR from hot S_1 states to a cold S_1 state, but then emit the remaining energy as fluorescence: so overall they convert little energy to optoacoustic signal (**Fig 1a**).

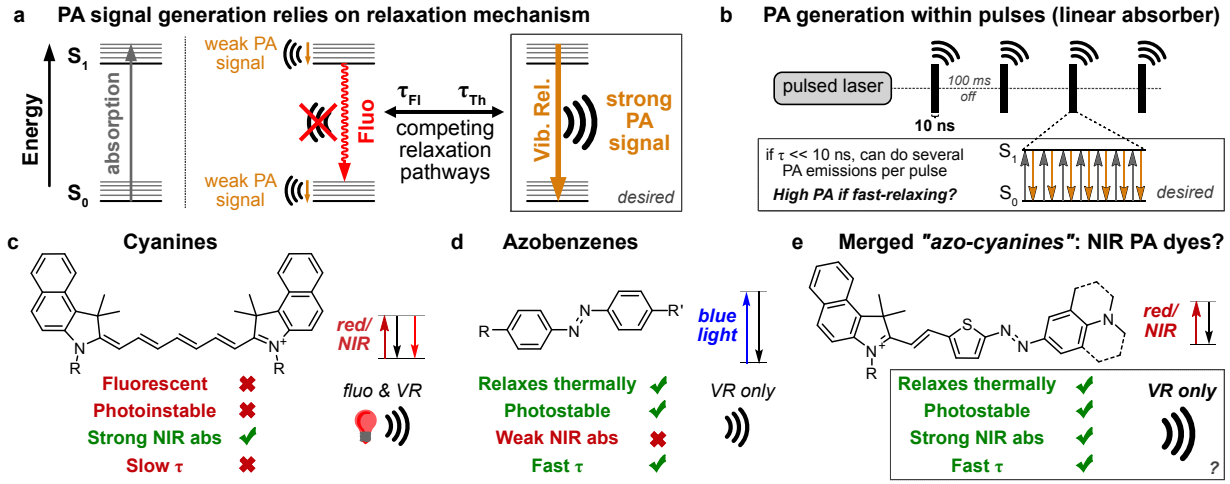

Figure 1. Design concept for molecular switch-based optoacoustic contrast agents. **(a)** Energy dissipated as heat contributes to PA signal (internal conversion then vibrational relaxation); fluorescence does not. **(b)** PA excitation is pulsed. For a linear absorber ($S_1 \rightarrow S_0$ relaxation halflife τ much shorter than the pulse), several $S_0 \rightarrow S_1 \rightarrow S_0$ excitation-relaxation cycles are possible within one pulse. **(c)** Cyanine dyes have strong NIR absorption, but are poor PA agents as they are slow-relaxing and non-photostable. **(d)** Azobenzenes have ultrafast nonradiative relaxation, but as UV/Vis-absorbers they are not useful for NIR PA. **(e) Hypothesis:** merging azobenzenes and cyanines should give strong, photostable NIR-absorbing PA emitters.

Yet, most NIR fluorophores are "bad," in the sense that their quantum yields are already low (e.g. 10%): so further lowering[21–24] or fully quenching[25–27] fluorescence can only increase PA signal by 10%, unless other mechanisms are also involved.[28] Two such mechanisms for PA enhancement are possible, and were well outlined by Rochford[20]. In brief, since PA supplies energy during infrequent excitation pulses that have similar duration as typical S_1 state lifetimes (pulses ~ ns, ~10 Hz repeat rate), time-dependent effects become important:

(1) If S_1 states can be excited further to S_n states during a PA pulse, these typically vibrationally relax rapidly back to S_1. The fast $S_1 \rightarrow S_n \rightarrow S_1$ cycles of such "**RSA**" chromophores (reverse-saturable absorbers) can thus allow higher PA signal than ordinary chromophores which use $S_0 \rightarrow S_1 \rightarrow S_0$ cycles ("SA", saturable absorbers). RSAs have been widely reported in PA studies *in vitro*.[20] However, further excitation depends non-linearly on (high) laser fluence; and within biologically-allowed energy limits, RSAs are outperformed by ordinary PA emitters that simply absorb light more strongly.[29,30] We also argue that cycling RSAs between S_1/S_n states may cause photoreactive damage to the chromophore or to biological tissues.

(2) Alternatively, if S_1 becomes very short-lived (lifetime << laser pulse length), many $S_0 \rightarrow S_1 \rightarrow S_0$ excitation/VR cycles become possible in a single pulse, so increasing the optoacoustic signal (**Fig 1b**). Rochford named such chromophores "**LAs**" (linear absorbers), since their PA signal response should scale linearly to the excitation intensity, although only one was identified: the genotoxic 580 nm-absorbing dye crystal violet.[20,31] We argue that if NIR LAs can be made, they hold the key to successful molecular PA, for two sets of reasons that we did not yet find collected in one place:

(2a) A major drawback of NIR fluorophores currently used in PA is their photoinstability; a typical case is **ICG** (**Fig 1c**), which offers only ~10^3 excitations before bleach-out (e.g. **Fig 3d**).[32,33] Thus, they cannot be used in imaging for longer than minutes, and their signal is not quantitative for their concentration, but only their surviving fraction. Instead, LAs should be very photostable, because rapid depletion of S_1 prevents excited-state photoreactivity pathways: thus LAs should allow long-term / longitudinal imaging, with accurate signal quantification, as is needed for molecular PA imaging.

(2b) LAs should give a predictable, useful response in biology, since they suffer only proportional signal decrease as the excitation power attenuates with depth (contrast this to nonlinear response of RSAs).

We recognised that molecular switches such as azobenzenes, which $S_1 \rightarrow S_0$ relax with picosecond halftimes and which, accordingly, have been exploited as enormously photostable dyes since >170 years,[34,35] would be an ideal LA chemotype; and that this parallels Rochford's recognition of crystal violet (a molecular rotor) as an excellent LA. There were encouraging hints that *appropriate* azobenzenes could succeed in PA. The non-emissivity and photostability of azobenzenes makes them popular as fluorescence quenchers in FRET probes, if excitation energy can be transferred onto them;[36] and in Gambhir's early work on acoustogenic probes, the complex azobenzene **BHQ3** was by chance found to be an "unusually strong" PA emitter, although the reasons for this were not explored and the work was not pursued further.[28] However, we knew of no biocompatible / water-soluble azobenzenes absorbing suitably in the ideal NIR window for PA (760-880 nm)[37] that could be tested (**Fig 1d**).

We now show the feasibility of rationally creating LA-type, NIR-absorbing, highly photostable and loud PA chromophores allowing multiple excitations per pulse, by uniting good chromophores and good switches. Our proof of principle work unites the NIR absorption of Cy dyes (strong chance to enter S_1) with the relaxation of azobenzene-type molecular switches (for ultrafast $S_1 \rightarrow S_0$) (**Fig 1e**).

RESULTS AND DISCUSSION

Design, synthesis, and spectral properties

Our first approach was to attach the phenylazo switch onto Cy5/7 fluorophores, at the middle (**M-AzCy5**) or the end (**E-AzCy5/7**) (**Fig 2**). In the second approach, we replaced part of the π-system with the azobenzene, imagining that conjugating over its N=N would maximise relaxation rates. This gave azo-hemicyanines, with phenylazobenzene systems of two π-system lengths (**P-AzHCy1/2**). Similarly to Nakamura, who used thiophenylazo bridges for redshifting,[38] we also tested two thiophenylazo systems, varying the donor groups (**T-AzHCy1/2**). Interestingly, Swager had suggested to use such scaffolds for PA imaging,[39] but the lack of water solubility had presumably blocked it. To force water solubility, we also installed an extra sulfonate in **wsT-AzHCy** (**Fig 2**).

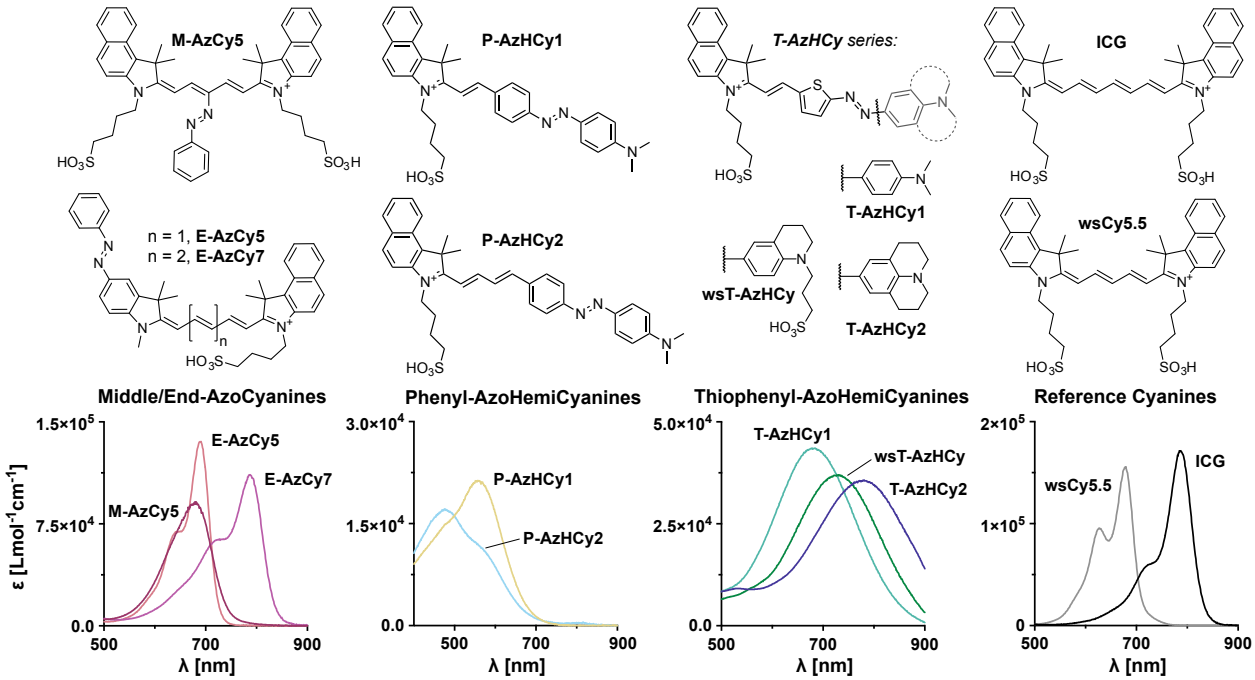

Figure 2. Structures and absorption spectra of azo-cyanines.

Their syntheses were direct. The middle phenylazo was installed by reacting the pentamethine with phenyldiazonium (**M-AzCy5**)[40]; the end phenylazos were installed onto the indolenin before the polymethines were synthesised by asymmetric Cy dye syntheses (**E-AzCy5/7**) (**Scheme S1**). The azo-hemicyanines were synthesised by Knoevenagel condensation of the indolene and the aldehydes (**P/T-AzHCy1/2**, **wsT-AzHCy**; **Scheme S2**).

The first requirement for these dyes was to reach strong NIR absorption, with λ_{max} desired as > 720 nm for *in vivo* applicability. Middle/end azo-cyanine **M/E-AzCy**s had similar absorption as the reference pentamethine **wsCy5.5** or heptamethine **ICG**, though were broadened and at lower intensity, as expected[41,42]. The phenylazo-hemicyanine **P-AzHCy** types absorb in the cyan/green, so were not continued for further study. Pleasingly, the thiophenylazo-hemicyanine **T-AzHCy** types had strong absorption in the PA-adapted NIR window, with **T-AzHCy2**'s λ_{max} of 779 nm being directly comparable to **ICG**; though again, their bands were broader and had lower extinction coefficients than the symmetric Cy dyes (**Fig 2, Table 1**).

Table 1. Absorption (1:1 EtOH:PBS) and fluorescence (EtOH)

	λ_{max} [nm]	ε [$\times 10^3$ $M^{-1}cm^{-1}$]	FWHM [nm]	Φ_{FL}
M-AzCy5	678	94	100	<0.01
E-AzCy5	689	136	72	0.22
E-AzCy7	785	111	114	0.10
P-AzHCy1	557	48	162	*not tested*
P-AzHCy2	483	28	245	*not tested*
T-AzHCy1	685	44	189	$<10^{-3}$
T-AzHCy2	779	35	220	$<10^{-3}$
wsT-AzHCy	729	37	199	$<10^{-3}$
wsCy5.5	*679*	*156*	*82*	*0.31*
ICG	*787*	*172*	*56*	*0.13 (lit.[43])*

The next requirement was to reach LA-type PA agents, by forcing a ultrashort-lived S_1 state. Low fluorescence is a necessary but insufficient proof of a short S_1 lifetime. The **T-AzHCy** types had zero detectable fluorescence on our usual setup; **M-AzCy5** was almost non-fluorescent, but Φ_{FL} of **E-AzCy5/7** barely differed from their parents (**Table 1**; we return to the S_1 lifetimes later, at **Table 2**).

Azobenzenes can undergo E⇄Z photoisomerizations[44] that change their absorption profiles. For quantifying a PA contrast agent, such changes would be an undesirable. We tested the **T-AzHCy** types that were now our leads, and these did not change Vis/NIR absorption under strong LED illumination, which is promising but not yet conclusive (discussion at **Fig S2**, see also TA spectroscopy below).

Optoacoustic Signal and Stability

We then tested our hypothesis that azo-merged-cyanines with fast $S_1 \rightarrow S_0$ VR would have strong, photostable, optoacoustic signals.

We first determined PA response spectra. Pleasingly, the **T-AzHCy**s and **M-AzCy** gave much stronger PA than **ICG** across broad spectral ranges, despite all being tested at the same optical density: an indication that they function as LAs, not SAs (**Fig 3a**). For an ideal and quantitative LA, the photoacoustic response spectrum should match the absorption spectrum: and indeed, they had perfect spectral overlay, which suits them as scaffolds for strong, linear, quantitative PA imaging over a range of wavelengths (**Fig S3**; a counterexample is provided by SA **ICG**, whose spectra differ strongly; contributing to its PA response being nonlinear and environment-dependent).[45]

To quantify the PA signal generation efficacy (SGE) robustly, we determined the PA-to-OD fits across the full OD range 0.1-0.5, which were linear for all species (**Fig S4**). Pleasingly, **wsT-AzHCy** and **T-AzHCy2** were excellently strong PA emitters, with SGE >3 times that of **ICG**. **M-AzCy5** was also a very strong PA emitter; **E-AzCy5/7** had the lowest SGE, similar to **ICG** (**Fig 3b**).

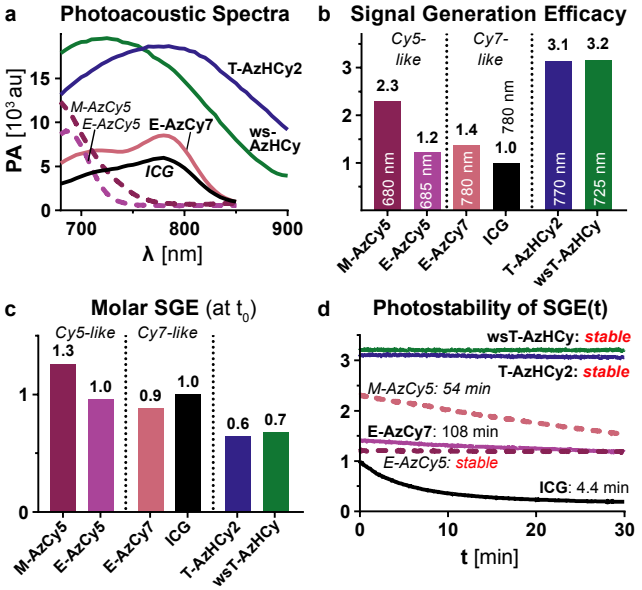

Figure 3. Optoacoustic properties. (**a**) Photoacoustic spectra at OD = 0.5 at λ_{max} in 1:1 PBS:EtOH. (**b**) PA signal generation efficacy (SGE) at constant OD, showing relative dye "loudness". (**c**) SGE adjusted to constant molarity (**ICG** set to 1). (**d**) PA photostability determination.

Noteworthily, these PA signal enhancements up to +220% (**Fig 3b**) far surpass the +10% expected from pure fluorescence quenching, so they support the desired multiple-excitations-per-pulse mechanism. If the SGEs are normalised not to constant OD but rather by molarity, as for enzyme-sensing molecular PA agents in biology, the lower extinction coefficients of the band-broadened azo-cyanines seem to diminish their signal (**Fig 3c**). Nevertheless, other factors are crucial for *in vivo* utility: mainly, whether the PA agent can be imaged stably over long time courses to deliver longitudinal information, without photobleaching that would render it non-quantitative.[7]

Therefore, we measured the stability and intensity of PA signal over time, under laser pulsing at 10 mJ/cm^2: a typical intensity for real-world applications (**Fig 3d**; at this energy, *in vivo* image acquisition can take seconds to minutes per section). The results support our LA design principle excellently. While the PA signal half-life ($t_{1/2}$) of **ICG** is only 4 min under these conditions, the **AzHCy**s simply do not bleach: a lowest possible bound for the halflife of **wsT-AzHCy** is 140 hours, i.e. >1900 times more stable than **ICG**; isoelectronic **T-AzHCy2** was similar (lowest bound 23 hours). The mid- and end-attached phenylazocyanines **M-AzCy5** and **E-AzCy5/7** were >10-fold more photostable than their cyanine congeners.

This direct access to **AzHCy** PA dyes that are "louder" at the start of imaging, then maintain their signal intensity for orders of magnitude longer than typical dyes, is the key value of our design. We believe it will be generally applicable to other dye families too, enabling them to withstand higher pulse energies in long-term imaging while maintaining higher signal intensity: which is particularly needed to image low-turnover enzyme activity, by accumulating signal over time.

Excited State Lifetimes and Evolution

The loud and photostable contrast agents we anticipated in these designs (**Fig 1e**) had now been validated experimentally. However, to test whether the mechanisms we had anticipated were operating, we wished to see if the excited state lifetimes for the new PA contrast agents had been shortened far below the laser pulse length, to enable the several excitations per pulse that the SGE data suggested. We thus performed time-resolved fluorescence spectroscopy[46] on a high-sensitivity setup, to capture the weak AzHCy fluorescence (spectra in **Fig S5**). The time-resolved fluorescence data were used to extract S_1 decay time constants (**Fig 4a**). Matching our hopes, the most photostable compounds **T-AzHCy2** and **wsT-AzHCy** relaxed electronically with ultrafast time constants τ_{PL} of just ~10 ps: which is 10^3-fold shorter than the PA laser pulse duration (10 ns). **M-AzCy5** and **E-AzCy5/7** had much longer time constants, ca. 540 and 370 ps respectively. This trend matches the involvement of the diazene in the π system (**T-AzHCy**: integral; **E/M-AzCy**: attached).

For multiple $S_0 \rightarrow S_1 \rightarrow S_0$ excitation/emission cycles per pulse, the depopulation of S_1 must be fast, as the luminescence data confirm, but the ground state must also be reached without other significant photoproducts.[20,29] We used transient absorption (TA) spectroscopy to study the excited state evolution. Pleasingly, both **T-AzHCy**s returned to the groundstate with ultrafast kinetics by a simple monoexponential $S_1 \rightarrow S_0$ path (τ_{TAS} ~ 4 ps; the slower species **M-AzCy5** takes a biexponential path with total halftime ~100 ps; **Fig 4b-d**, **Fig S7**). Although acquired in different solvents, the TA and luminescence lifetimes match closely. Thus, our "star" species show the full set of properties we had targeted for loud, linear PA emitters (**Table 2**): ultrafast excited state decay to the groundstate allowing multiple $S_0 \rightarrow S_1 \rightarrow S_0$ cycles per pulse, associated to outstanding photostability and excellent SGE, just as desired for easy and reliable quantification in NIR optoacoustic imaging.

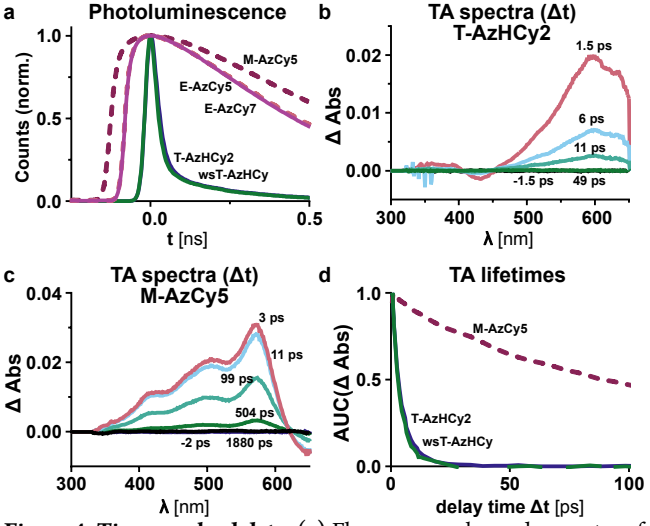

Figure 4. Time-resolved data. (**a**) Fluorescence shows decay rates of singlet excited states. (**b-d**) Transient absorption (TA) spectroscopy: **T-AzHCy2** relaxes fully to S_0 with τ_{TAS} ~4 ps, but **M-AzCy5** has τ_{TAS} ~180 ps. (**d**) TA ΔAbs decays (fitted lifetimes given in **Table 2**).

Table 2. Summary of Key Optoacoustic Parameters

	photoacoustic response			elec. relaxation	
	λ_{SGE} [nm]	SGE	stability $t_{1/2}$ [min]	τ_{PL}[a] [ps]	τ_{TAS} [ps]
M-AzCy5	680	2.3	54	540[b]	180[b]
E-AzCy5	685	1.2	≫4270[c]	386[b]	*not m.*
E-AzCy7	785	1.4	108	363	*not m.*
T-AzHCy2	770	3.1	≫1400[c]	13	4.0
wsT-AzHCy	740	3.2	≫8400[c]	9	3.6
***ICG** (ref.)*	*780*	*1*	*4.4*	*10*[3; d]	*not m.*

[a] major decay; [b] complex fit; [c] lower bounds; [d] value from ref[43]; "*not m.*": not measured.

CONCLUSION

The great advances in biology have in large part been driven by chemical chromophores. Fluorophores, which easily enable quantitative imaging of live cell enzymatic activity, have for several decades been tuned e.g. for shallow *in vivo* imaging.[47] The equipment and engineering necessary to instead harness chromophores' optoacoustic response for deep *in vivo* imaging is now becoming available. Yet, to realise its promise for quantitative imaging in live animal as well as clinical settings, we must move beyond repurposing poorly-adapted contrast agents such as fluorophores: we must rationally develop chemical design strategies for optoacoustic chromophores, tailored to the unique challenges and opportunities of PA.

Here, we have focused on the $S_1 \rightarrow S_0$ lifetime: one of the most powerful photophysical regulators of PA contrast agent performance, but also one which has been chemically almost ignored.

We showed that the rational integration of molecular switches into NIR-absorbing scaffolds can accelerate their $S_1 \rightarrow S_0$ transition by >100-fold. This gives a >1000-fold enhancement of PA signal photostability, while also converting even poorly quantifiable "saturable absorber" chromophores into "linear absorber" PA contrast agents that promise to be reliably and stably quantifiable at arbitrary illumination intensity, over arbitrarily long imaging timecourses. By permitting many $S_0 \rightarrow S_1 \rightarrow S_0$ cycles per pulse, **AzHCy** offer a simple organic chromophore method to multiply PA signal response: and even on current standard PA equipment, with relatively long pulse settings that are optimised around the weaknesses of current SAs, these ultrafast-relaxing **AzHCy** agents already provide 3-fold higher signal generation efficacy at the start of imaging. Their linear response to excitation intensity is however an opportunity to harness shorter excitation pulses to deliver the same PA output, but with vastly higher spatial resolution (smaller excitation voxel size): which no current NIR-active organic PA contrast agents can provide.

As this rational design hypothesis succeeded so directly, we predict that remastering molecular switches will become a powerful route to enhance chromophores' photophysically-determined performance features, in a truly general sense. For example, the broadened NIR absorption of the nonfluorescent **AzHCy**s (beyond 900 nm for **T-AzHCy2**, and easily tunable) makes them ideal candidate NIR fluorescence quenchers (another molecularly-underrepresented class of imaging agent) e.g. for off→ON, NIR, FRET probes. PA also faces other challenges for engineering the photophysics and biocompatibility of its chromophores,[20] but we believe that they too can be solved in a modular way that can synergise with the benefits of ultrafast relaxation. Perhaps the most significant of these, is to introduce enzyme-responsive[48,49] molecular PA imaging for the NIR/SWIR region.[50] In this respect, Schnermann's enzyme-activatable NIR cyanine template (CyBam)[51] may offer an ideal model system to synergise with the arylazo-cyanines developed here. We are convinced that the scope for other chromophore types, as well as other chemotypes of switches, rotors, or motors, will be broad enough to power much creative harmony: in optoacoustics and beyond.

ASSOCIATED CONTENT

Supporting Information

The Supporting Information is available free of charge on the ACS Publications website.

Synthesis, photophysics data, and NMR spectra (PDF).

AUTHOR INFORMATION

Corresponding Author

*Oliver Thorn-Seshold – *Department of Pharmacy, Ludwig- Maximilians University of Munich, Munich 81377, Germany;*
orcid.org/0000-0003-3981-651X;
Email: oliver.thorn-seshold@cup.lmu.de

Authors

All authors have given approval to the final version of the manuscript.

Funding

This research was supported by funds from the Boehringer Ingelheim Stiftung (Exploration Grant to O.T.-S.) and the German Research Foundation (DFG: Emmy Noether grant number 400324123 to O.T.-S.; SFB 1032 number 201269156 project B09 to O.T.-S.; SFB TRR 152 number 239283807 project P24 to O.T.-S.; and SPP 1926 number 426018126 project XVIII to O.T.-S.).

Notes

The authors declare no competing financial interest.

ACKNOWLEDGMENTS

We thank Michaela Kaltenegger and Jan Prohaska (LMU) for synthetic support and cordial discussions; Viktorija Glembockyte (LMU) for mechanistic discussions and advice on photophysical applications; and Eberhard Riedle (LMU) for motivation and discussions around using transient absorption spectroscopy for mechanistic studies.

ABBREVIATIONS

IC, internal conversion; LA, linear absorber; MSOT, multispectral optoacoustic (or photoacoustic) tomography; NIR, near-infrared; PA, photoacoustic (or optoacoustic) imaging; RSA, reverse-saturable absorber; SA, saturable absorber; VR, vibrational relaxation.

REFERENCES

(1) Ntziachristos, V. Going Deeper than Microscopy: The Optical Imaging Frontier in Biology. *Nat Methods* **2010**, *7* (8), 603–614. https://doi.org/10.1038/nmeth.1483.

(2) Ntziachristos, V.; Razansky, D. Molecular Imaging by Means of Multispectral Optoacoustic Tomography (MSOT). *Chem. Rev.* **2010**, *110* (5), 2783–2794. https://doi.org/10.1021/cr9002566.

(3) Taruttis, A.; Ntziachristos, V. Advances in Real-Time Multispectral Optoacoustic Imaging and Its Applications. *Nat. Photon* **2015**, *9* (4), 219–227. https://doi.org/10.1038/nphoton.2015.29.

(4) Karlas, A.; Pleitez, M. A.; Aguirre, J.; Ntziachristos, V. Optoacoustic Imaging in Endocrinology and Metabolism. *Nat Rev Endocrinol* **2021**, *17* (6), 323–335. https://doi.org/10.1038/s41574-021-00482-5.

(5) Moore, C.; Jokerst, J. V. Strategies for Image-Guided Therapy, Surgery, and Drug Delivery Using Photoacoustic Imaging. *Theranostics* **2019**, *9* (6), 1550–1571. https://doi.org/10.7150/thno.32362.

(6) Jacques, S. L. Optical Properties of Biological Tissues: A Review. *Phys. Med. Biol.* **2013**, *58* (11), R37–R61. https://doi.org/10.1088/0031-9155/58/11/R37.

(7) Gujrati, V.; Mishra, A.; Ntziachristos, V. Molecular Imaging Probes for Multi-Spectral Optoacoustic Tomography. *Chem. Commun.* **2017**, *53* (34), 4653–4672. https://doi.org/10.1039/C6CC09421J.

(8) Gorka, A. P.; Nani, R. R.; Schnermann, M. J. Harnessing Cyanine Reactivity for Optical Imaging and Drug Delivery. *Acc. Chem. Res.* **2018**, *51* (12), 3226–3235. https://doi.org/10.1021/acs.accounts.8b00384.

(9) Beziere, N.; Lozano, N.; Nunes, A.; Salichs, J.; Queiros, D.; Kostarelos, K.; Ntziachristos, V. Dynamic Imaging of PEGylated Indocyanine Green (ICG) Liposomes within the Tumor Microenvironment Using Multi-Spectral Optoacoustic Tomography (MSOT). *Biomaterials* **2015**, *37*, 415–424. https://doi.org/10.1016/j.biomaterials.2014.10.014.

(10) Zhong, J.; Yang, S.; Zheng, X.; Zhou, T.; Xing, D. In Vivo Photoacoustic Therapy with Cancer-Targeted Indocyanine Green-Containing

Nanoparticles. *Nanomedicine* **2013**, *8* (6), 903–919. https://doi.org/10.2217/nnm.12.123.

(11) Cosco, E. D.; Caram, J. R.; Bruns, O. T.; Franke, D.; Day, R. A.; Farr, E. P.; Bawendi, M. G.; Sletten, E. M. Flavylium Polymethine Fluorophores for Near- and Shortwave Infrared Imaging. *Angew. Chem. Int. Ed.* **2017**, *56* (42), 13126–13129. https://doi.org/10.1002/anie.201706974.

(12) Cosco, E. D.; Spearman, A. L.; Ramakrishnan, S.; Lingg, J. G. P.; Saccomano, M.; Pengshung, M.; Arús, B. A.; Wong, K. C. Y.; Glasl, S.; Ntziachristos, V.; Warmer, M.; McLaughlin, R. R.; Bruns, O. T.; Sletten, E. M. Shortwave Infrared Polymethine Fluorophores Matched to Excitation Lasers Enable Non-Invasive, Multicolour in Vivo Imaging in Real Time. *Nat. Chem.* **2020**, *12* (12), 1123–1130. https://doi.org/10.1038/s41557-020-00554-5.

(13) Bandi, V. G.; Luciano, M. P.; Saccomano, M.; Patel, N. L.; Bischof, T. S.; Lingg, J. G. P.; Tsrunchev, P. T.; Nix, M. N.; Ruehle, B.; Sanders, C.; Riffle, L.; Robinson, C. M.; Difilippantonio, S.; Kalen, J. D.; Resch-Genger, U.; Ivanic, J.; Bruns, O. T.; Schnermann, M. J. Targeted Multicolor in Vivo Imaging over 1,000 nm Enabled by Nonamethine Cyanines. *Nat Methods* **2022**, *19* (3), 353–358. https://doi.org/10.1038/s41592-022-01394-6.

(14) Yuan, L.; Lin, W.; Yang, Y.; Chen, H. A Unique Class of Near-Infrared Functional Fluorescent Dyes with Carboxylic-Acid-Modulated Fluorescence ON/OFF Switching: Rational Design, Synthesis, Optical Properties, Theoretical Calculations, and Applications for Fluorescence Imaging in Living Animals. *J. Am. Chem. Soc.* **2012**, *134* (2), 1200–1211. https://doi.org/10.1021/ja209292b.

(15) Li, H.; Kim, H.; Xu, F.; Han, J.; Yao, Q.; Wang, J.; Pu, K.; Peng, X.; Yoon, J. Activity-Based NIR Fluorescent Probes Based on the Versatile Hemicyanine Scaffold: Design Strategy, Biomedical Applications, and Outlook. *Chem. Soc. Rev.* **2022**, *51* (5), 1795–1835. https://doi.org/10.1039/D1CS00307K.

(16) Lucero, M. Y.; Chan, J. Photoacoustic Imaging of Elevated Glutathione in Models of Lung Cancer for Companion Diagnostic Applications. *Nat. Chem.* **2021**, *13* (12), 1248–1256. https://doi.org/10.1038/s41557-021-00804-0.

(17) Gardner, S. H.; Brady, C. J.; Keeton, C.; Yadav, A. K.; Mallojjala, S. C.; Lucero, M. Y.; Su, S.; Yu, Z.; Hirschi, J. S.; Mirica, L. M.; Chan, J. A General Approach to Convert Hemicyanine Dyes into Highly Optimized Photoacoustic Scaffolds for Analyte Sensing. *Angew. Chem. Int. Ed.* **2021**, *60* (34), 18860–18866. https://doi.org/10.1002/anie.202105905.

(18) Zhang, S.; Chen, H.; Wang, L.; Qin, X.; Jiang, B.-P.; Ji, S.-C.; Shen, X.-C.; Liang, H. A General Approach to Design Dual Ratiometric Fluorescent and Photoacoustic Probe for Quantitatively Visualizing Tumor Hypoxia Levels in Vivo. *Angew. Chem. Int. Ed.* **2021**, *61*, e202107076. https://doi.org/10.1002/ange.202107076.

(19) Weber, J.; Beard, P. C.; Bohndiek, S. E. Contrast Agents for Molecular Photoacoustic Imaging. *Nat. Methods* **2016**, *13* (8), 639–650. https://doi.org/10.1038/nmeth.3929.

(20) Hatamimoslehabadi, M.; Bellinger, S.; La, J.; Ahmad, E.; Frenette, M.; Yelleswarapu, C.; Rochford, J. Correlation of Photophysical Properties with the Photoacoustic Emission for a Selection of Established Chromophores. *J. Phys. Chem. C* **2017**, *121* (43), 24168–24178. https://doi.org/10.1021/acs.jpcc.7b07598.

(21) Rathnamalala, C. S. L.; Pino, N. W.; Herring, B. S.; Hooper, M.; Gwaltney, S. R.; Chan, J.; Scott, C. N. Thienylpiperidine Donor NIR Xanthene-Based Dye for Photoacoustic Imaging. *Org. Lett.* **2021**, *23* (19), 7640–7644. https://doi.org/10.1021/acs.orglett.1c02862.

(22) Liu, N.; Gujrati, V.; Malekzadeh-Najafabadi, J.; Werner, J. P. F.; Klemm, U.; Tang, L.; Chen, Z.; Prakash, J.; Huang, Y.; Stiel, A.; Mettenleiter, G.; Aichler, M.; Blutke, A.; Walch, A.; Kleigrewe, K.; Razansky, D.; Sattler, M.; Ntziachristos, V. Croconaine-Based Nanoparticles Enable Efficient Optoacoustic Imaging of Murine Brain Tumors. *Photoacoustics* **2021**, *22*, 100263. https://doi.org/10.1016/j.pacs.2021.100263.

(23) Liu, N.; O'Connor, P.; Gujrati, V.; Gorpas, D.; Glasl, S.; Blutke, A.; Walch, A.; Kleigrewe, K.; Sattler, M.; Plettenburg, O.; Ntziachristos, V. Facile Synthesis of a Croconaine-Based Nanoformulation for Optoacoustic Imaging and Photothermal Therapy. *Adv. Healthc. Mater.* **2021**, *10* (9), 2002115. https://doi.org/10.1002/adhm.202002115.

(24) Zhou, X.; Fang, Y.; Wimalasiri, V.; Stains, C. I.; Miller, E. W. A Long-Wavelength Xanthene Dye for Photoacoustic Imaging. *Chem. Commun.* **2022**, *58* (85), 11941–11944. https://doi.org/10.1039/D2CC03947H.

(25) Ikeno, T.; Hanaoka, K.; Iwaki, S.; Myochin, T.; Murayama, Y.; Ohde, H.; Komatsu, T.; Ueno, T.; Nagano, T.; Urano, Y. Design and Synthesis of an Activatable Photoacoustic Probe for Hypochlorous Acid. *Anal. Chem.* **2019**, *91* (14), 9086–9092. https://doi.org/10.1021/acs.analchem.9b01529.

(26) Merkes, J. M.; Lammers, T.; Kancherla, R.; Rueping, M.; Kiessling, F.; Banala, S. Tuning Optical Properties of BODIPY Dyes by Pyrrole Conjugation for Photoacoustic Imaging. *Adv. Opt. Mater.* **2020**, *8* (11), 1902115. https://doi.org/10.1002/adom.201902115.

(27) Laramie, M.; Smith, M.; Marmarchi, F.; McNally, L.; Henary, M. Small Molecule Optoacoustic Contrast Agents: An Unexplored Avenue for Enhancing In Vivo Imaging. *Molecules* **2018**, *23* (11), 2766. https://doi.org/10.3390/molecules23112766.

(28) Levi, J.; Kothapalli, S. R.; Ma, T.-J.; Hartman, K.; Khuri-Yakub, B. T.; Gambhir, S. S. Design, Synthesis, and Imaging of an Activatable Photoacoustic Probe. *J. Am. Chem. Soc.* **2010**, *132* (32), 11264–11269. https://doi.org/10.1021/ja104000a.

(29) Frenette, M.; Hatamimoslehabadi, M.; Bellinger-Buckley, S.; Laoui, S.; La, J.; Bag, S.; Mallidi, S.; Hasan, T.; Bouma, B.; Yelleswarapu, C.; Rochford, J. Shining Light on the Dark Side of Imaging: Excited State Absorption Enhancement of a Bis-Styryl BODIPY Photoacoustic Contrast Agent. *J. Am. Chem. Soc.* **2014**, *136* (45), 15853–15856. https://doi.org/10.1021/ja508600x.

(30) Borg, R. E.; Hatamimoslehabadi, M.; Bellinger, S.; La, J.; Mithila, F.; Yelleswarapu, C.; Rochford, J. Photophysical and Photoacoustic Properties of π-Extended Curcumin Dyes. Effects of the Terminal Dimethylamino Electron-Donor and the Bridging Aryl Ring. *Photochem. Photobiol.* **2019**, *95* (1), 280–292. https://doi.org/10.1111/php.12980.

(31) Borg, R. E.; Rochford, J. Molecular Photoacoustic Contrast Agents: Design Principles & Applications. *Photochem. Photobiol.* **2018**, *94* (6), 1175–1209. https://doi.org/10.1111/php.12967.

(32) Matikonda, S. S.; Helmerich, D. A.; Meub, M.; Beliu, G.; Kollmannsberger, P.; Greer, A.; Sauer, M.; Schnermann, M. J. Defining the Basis of Cyanine Phototruncation Enables a New Approach to Single-Molecule Localization Microscopy. *ACS Cent. Sci.* **2021**, *7* (7), 1144–1155. https://doi.org/10.1021/acscentsci.1c00483.

(33) Nani, R. R.; Kelley, J. A.; Ivanic, J.; Schnermann, M. J. Reactive Species Involved in the Regioselective Photooxidation of Heptamethine Cyanines. *Chem. Sci.* **2015**, *6* (11), 6556–6563. https://doi.org/10.1039/C5SC02396C.

(34) Bandara, H. M. D.; Burdette, S. C. Photoisomerization in Different Classes of Azobenzene. *Chem. Soc. Rev.* **2012**, *41* (5), 1809–1825. https://doi.org/10.1039/C1CS15179G.

(35) Garcia-Amorós, J.; Maerz, B.; Reig, M.; Cuadrado, A.; Blancafort, L.; Samoylova, E.; Velasco, D. Picosecond Switchable Azo Dyes. *Chem. Eur. J.* **2019**, *25* (32), 7726–7732. https://doi.org/10.1002/chem.201900796.

(36) Chevalier, A.; Massif, C.; Renard, P.-Y.; Romieu, A. Bioconjugatable Azo-Based Dark-Quencher Dyes: Synthesis and Application to Protease-Activatable Far-Red Fluorescent Probes. *Chem. Eur. J.* **2013**, *19* (5), 1686–1699. https://doi.org/10.1002/chem.201203427.

(37) Dong, M.; Babalhavaeji, A.; Samanta, S.; Beharry, A. A.; Woolley, G. A. Red-Shifting Azobenzene Photoswitches for in Vivo Use. *Acc. Chem. Res.* **2015**, *48* (10), 2662–2670. https://doi.org/10.1021/acs.accounts.5b00270.

(38) Fuse, S.; Oishi, T.; Matsumura, K.; Hayashi, Y.; Kawauchi, S.; Nakamura, H. Design, Synthesis, and Evaluation of Azo D–π-A Dyes as Photothermal Agents. *Org. Biomol. Chem.* **2019**, *18* (1), 93–101. https://doi.org/10.1039/C9OB02066G.

(39) Swager, T. M.; Delage-Laurin, L. From Light to Heat: Synthesis of Azo D-π-A Dyes as Photothermal Agents. *Synfacts* **2020**, *16* (02), 0152. https://doi.org/10.1055/s-0039-1691650.

(40) Treibs, A.; Zimmer-Galler, R. Azokupplung von Pyrrol- und Cyaninfarbstoffen. *Justus Liebigs Annalen der Chemie* **1959**, *627* (1), 166–181. https://doi.org/10.1002/jlac.19596270117.

(41) Tolbert, L. M.; Zhao, X. Beyond the Cyanine Limit: Peierls Distortion and Symmetry Collapse in a Polymethine Dye. *J. Am. Chem. Soc.* **1997**, *119* (14), 3253–3258. https://doi.org/10.1021/ja9626953.

(42) Pascal, S.; Haefele, A.; Monnereau, C.; Charaf-Eddin, A.; Jacquemin, D.; Le Guennic, B.; Andraud, C.; Maury, O. Expanding the Polymethine Paradigm: Evidence for the Contribution of a Bis-Dipolar Electronic Structure. *J. Phys. Chem. A* **2014**, *118* (23), 4038–4047. https://doi.org/10.1021/jp501358q.

(43) Berezin, M. Y.; Achilefu, S. Fluorescence Lifetime Measurements and Biological Imaging. *Chem. Rev.* **2010**, *110* (5), 2641–2684. https://doi.org/10.1021/cr900343z.

(44) Hartley, G. S. The Cis-Form of Azobenzene. *Nature* **1937**, *140* (3537), 281–281. https://doi.org/10.1038/140281a0.

(45) Fuenzalida Werner, J. P.; Huang, Y.; Mishra, K.; Janowski, R.; Vetschera, P.; Heichler, C.; Chmyrov, A.; Neufert, C.; Niessing, D.; Ntziachristos, V.; Stiel, A. C. Challenging a Preconception: Optoacoustic Spectrum Differs from the Optical Absorption Spectrum of Proteins and Dyes for Molecular Imaging. *Anal. Chem.* **2020**, *92* (15), 10717–10724. https://doi.org/10.1021/acs.analchem.0c01902.

(46) DiFrancesco, M. L.; Lodola, F.; Colombo, E.; Maragliano, L.; Bramini, M.; Paternò, G. M.; Baldelli, P.; Serra, M. D.; Lunelli, L.; Marchioretto, M.; Grasselli, G.; Cimò, S.; Colella, L.; Fazzi, D.; Ortica, F.; Vurro, V.; Eleftheriou, C. G.; Shmal, D.; Maya-Vetencourt, J. F.; Bertarelli, C.; Lanzani, G.; Benfenati, F. Neuronal Firing Modulation by a Membrane-Targeted Photoswitch. *Nat. Nanotechnol.* **2020**, *15* (4), 296–306. https://doi.org/10.1038/s41565-019-0632-6.

(47) Grimm, J. B.; Lavis, L. D. Caveat Fluorophore: An Insiders' Guide to Small-Molecule Fluorescent Labels. *Nat Methods* **2022**, *19* (2), 149–158. https://doi.org/10.1038/s41592-021-01338-6.

(48) Kobayashi, H.; Ogawa, M.; Alford, R.; Choyke, P. L.; Urano, Y. New Strategies for Fluorescent Probe Design in Medical Diagnostic Imaging. *Chem. Rev.* **2010**, *110* (5), 2620–2640. https://doi.org/10.1021/cr900263j.

(49) Brøndsted, F.; Fang, Y.; Zhou, X.; Stains, C. *Engineering Phosphinate-Containing Rhodamines for Turn-On Photoacoustic Imaging Applications*; preprint; Chemistry, 2023. https://doi.org/10.26434/chemrxiv-2023-w8x3c.

(50) Zhao, Z.; Swartchick, C. B.; Chan, J. Targeted Contrast Agents and Activatable Probes for Photoacoustic Imaging of Cancer. *Chem. Soc. Rev.* **2022**. https://doi.org/10.1039/D0CS00771D.

(51) Usama, S. M.; Inagaki, F.; Kobayashi, H.; Schnermann, M. J. Norcyanine-Carbamates Are Versatile Near-Infrared Fluorogenic Probes. *J. Am. Chem. Soc.* **2021**, *143* (15), 5674–5679. https://doi.org/10.1021/jacs.1c02112.

Graphic for Table of Contents (TOC):